

Impedance Representation of the S-matrix: Proton Structure and Spin from an Electron Model

Peter Cameron*
Strongarm Studios
Mattituck, NY USA 11952

(Dated: June 17, 2016)

The possibility of electron geometric structure is studied using a model based upon quantized electromagnetic impedances, written in the language of geometric Clifford algebra. The electron is expanded beyond the point, to include the simplest possible objects in one, two, and three dimensions. These point, line, plane, and volume elements, quantized at the scale of the electron Compton wavelength and given the attributes of electric and magnetic fields, comprise a minimally complete Pauli algebra of flat 3D space. One can calculate quantized impedances associated with elementary particle spectrum observables (the S-matrix) from interactions between the eight geometric objects of this algebra - one scalar, three vectors, three bivector pseudovectors, and one trivector pseudoscalar. The resulting matrix comprises a Dirac algebra of 4D spacetime. Proton structure and spin are extracted via the dual character of scalar electric and pseudoscalar magnetic charges.

INTRODUCTION

This paper focuses upon the primary problem of the high energy spin physics community, the ongoing failure of QCD point-particle quark models to provide a coherent picture of nucleon spin[1–4]. It is organized as follows:

- Introduction - outlines the structure of the paper, introduces the impedance representation, and gives a **guided tour of the figures**.
- Geometric Clifford Algebra and the Impedance Representation - presents a brief historical account of the remarkable absence from mainstream QFT of **Clifford’s original geometric interpretation**, identifies the fundamental geometric objects (FGOs) of the 3D Pauli and 4D Dirac subalgebras of geometric algebra (GA) with the FGOs of the impedance representation, and discusses topological symmetry breaking inherent in the algebras.
- S-matrix and the Impedance Representation - presents a brief historical account of the remarkable absence from mainstream QFT of **exact impedance quantization**, and the equivalence of the S-matrix and impedance representations of QFT.
- Dark Modes and Symmetry Breaking - mode structures of all the elementary particles are present in the impedance representation. Particles with **dark FGOs (magnetic charge, electric dipole and flux quantum)** decay/decohere due to the differing vacuum impedances they excite, and the resulting differential phase shifts. The stable proton contains no dark FGOs, permitting us to pick out its mode structure.
- Proton Structure - mode structure is discussed; transition modes and topological mass generation,

then the stable eigenmodes and their **representation of point particle quark models**.

- Proton Spin - the simple and exact spin 1/2 quantum that emerges from the algebra is identified.

Guided Tour of the Figures:

At the outset we proceed beyond point particles by examining commonality between fundamental geometric objects (FGOs) of geometric Clifford algebra[5–10] and the impedance model of the electron[11] (**figure 1**).

Commonality among the Fundamental Geometric Objects (FGOs)				
FGO	GA	IA	visible?	topology
point	scalar	electric charge	yes	one hole
line	vector	electric moment	no	two holes
line	vector	magnetic flux quantum	yes	two holes
surface	bivector	electric flux quantum	no	no hole
surface	bivector	magnetic moment	yes	no hole
volume	trivector	magnetic charge	no	no hole

FIG. 1. Shared FGOs of the 3D Pauli subalgebra of geometric Clifford algebra [8] and those of the impedance approach to geometric structure of the electron [11]. Bivector and trivector are pseudovector and pseudoscalar of the Pauli algebra.

As the figure shows, electromagnetic duality[12] results in magnetic inversion of geometric grade/dimension:

- scalar electric *charge* - grade 0 point
- vector electric *moment* - grade 1 line
- pseudovector magnetic *moment* - grade 2 area
- pseudoscalar magnetic *charge* - grade 3 volume

All are orientable.

These objects are identified with the eight FGOs of a minimally complete Pauli algebra of space (top and left of **figure 2**), and via geometric products (**figure 3**) generate an impedance representation of their interactions in the Dirac algebra of flat Minkowski spacetime[8].

	electric charge e scalar	electric moment 1 d_{E1} vector	electric moment 2 d_{E2} vector	mag flux quantum ϕ_B vector	elec flux quantum 1 ϕ_{E1} pseudovector	elec flux quantum 2 ϕ_{E2} pseudovector	magnetic moment μ_{Bohr} pseudovector	magnetic charge g pseudoscalar
e	ee ■ scalar	ed_{E1}	ed_{E2} vector	$e\phi_B$ ●	$e\phi_{E1}$ ▲	$e\phi_{E2}$ ▲ bivector	$e\mu_B$	eg pseudovector
d_{E1}	$d_{E1}e$	$d_{E1}d_{E1}$ ◆	$d_{E1}d_{E2}$	$d_{E1}\phi_B$	$d_{E1}\phi_{E1}$	$d_{E1}\phi_{E2}$	$d_{E1}\mu_B$	$d_{E1}g$
d_{E2}	$d_{E2}e$	$d_{E2}d_{E1}$	$d_{E2}d_{E2}$ ◆	$d_{E2}\phi_B$	$d_{E2}\phi_{E1}$	$d_{E2}\phi_{E2}$	$d_{E2}\mu_B$	$d_{E2}g$
ϕ_B	$\phi_B e$ ● vector	$\phi_B d_{E1}$	$\phi_B d_{E2}$ scalar + bivector	$\phi_B \phi_B$	$\phi_B \phi_{E1}$	$\phi_B \phi_{E2}$ vector + pseudovector	$\phi_B \mu_B$	$\phi_B g$ ▲ bivector
ϕ_{E1}	$\phi_{E1}e$ ▲	$\phi_{E1}d_{E1}$	$\phi_{E1}d_{E2}$	$\phi_{E1}\phi_B$	$\phi_{E1}\phi_{E1}$	$\phi_{E1}\phi_{E2}$	$\phi_{E1}\mu_B$	$\phi_{E1}g$ ●
ϕ_{E2}	$\phi_{E2}e$ ▲	$\phi_{E2}d_{E1}$	$\phi_{E2}d_{E2}$	$\phi_{E2}\phi_B$ ▼	$\phi_{E2}\phi_{E1}$	$\phi_{E2}\phi_{E2}$	$\phi_{E2}\mu_B$	$\phi_{E2}g$ ●
μ_B	$\mu_B e$ bivector	$\mu_B d_{E1}$	$\mu_B d_{E2}$ vector + pseudovector	$\mu_B \phi_B$	$\mu_B \phi_{E1}$	$\mu_B \phi_{E2}$ scalar + pseudoscalar	$\mu_B \mu_B$ ◆	$\mu_B g$ vector
g	ge pseudovector	gd_{E1}	gd_{E2} bivector	$g\phi_B$ ▲	$g\phi_{E1}$ ●	$g\phi_{E2}$ ● vector	$g\mu_B$	gg ■ scalar

FIG. 2. Impedance representation of the S-matrix. At top and left are the eight FGOs of both the impedance model[11] and a minimally complete Pauli algebra of 3D space - 1 scalar, 3 vectors, 3 bivectors/pseudovectors, and 1 trivector/pseudoscalar [8]. The matrix of background independent two-body interactions[13] is generated by geometric products of these FGOs. Matrix elements comprise a 4D Dirac algebra of flat Minkowski spacetime, arranged in even (blue) and odd (yellow) by geometric grade of the emerging FGOs (the observables). ‘Pauli FGOs’ enter an interaction. ‘Dirac FGOs’ emerge, are the Pauli FGOs entering the next interaction. Impedances of modes indicated by colored symbols are plotted as a function of energy/length scale in **figure 4**. Scale invariant mode impedances (quantum Hall, centrifugal, chiral, Coriolis, three body,...) are associated with inverse square potentials. They can do no work, but shift quantum phase, can act as mode couplers.

As explained in what follows, in the model there are two each electric dipole/vector and electric flux quantum/pseudovector. If we take the resulting eight FGOs at the top of **figure 2** to comprise the electron, then in the manner of the Dirac equation those on the left are the positron.

We then come back to point particles to set an anchor point in the common language of the theorist, namely the S-matrix representation of quantum field theory[14–20], and explain its equivalence with what we are calling the impedance representation. When you see ‘impedance’, think S-matrix [21]. This permits one to look between asymptotically free states of initial and final wavefunctions, to look deep inside the black box of Wheeler and Heisenberg’s ‘observables only’ S-matrix through the eyes of both experimentalists *and* theoreticians.

A portion of the network that results from calculating interaction impedances of ‘Pauli FGOs’ when endowed with electric and magnetic fields is shown in **figure 4**. The relationship between this representation and the unstable particle spectrum is established via correlations of particle lifetimes (their coherence lengths on the causal boundary of the light cone) with network nodes, where impedances are **matched** and energy flows without reflection (as required by the decay process) [22–24].

The *stable* proton is absent from **figure 4**, which includes only photon, electron, and all the *unstable* particles. Which is not to say it is absent from **figure 2**. If that figure is indeed a reasonable first approximation of nature’s S-matrix, then proton mode structure must be there. The question is how to identify those modes in the maze of possibilities present in the impedance matrix.

As shown in **figure 1**, we see electric charge and magnetic dipole and flux quantum, but not their duals [12]. Magnetic charge [25, 26] and electric dipole and flux quantum are absent, not visible, ‘dark’. Dark FGOs couple only indirectly to the photon not because they are too weak, but rather too strong (**figure 5**) [11].

The speed of light (or impedance of free space) can be calculated from excitation of virtual electron-positron pairs (represented in part as the impedance network of **figure 4**) by the photon[27]. Dark FGOs couple more strongly (see a different impedance). Modes containing one or more dark FGOs decohere from differential phase shifts. To identify the mode structure of the proton we need only consider modes comprised exclusively of visible FGOs (**figure 6**), a tremendous simplification.

GEOMETRIC CLIFFORD ALGEBRA AND THE IMPEDANCE REPRESENTATION

The impedance approach (IA) to the S-matrix is grounded in geometric Clifford algebra (GA), the algebra of interactions between geometric objects as originally conceived by Grassman and Clifford[5–10]. With the early death of Clifford in the late 1800s and ascendance of the more simple vector algebra of Gibbs, the power of geometric interpretation has for the most part been lost in modern theoretical physics. While both Pauli and Dirac algebras are subalgebras of GA, their geometric origin went unrecognized by their creators. It was only in the 1960s with the work of David Hestenes that the power of geometric interpretation was rediscovered and introduced to physics, as recognized by the American Physical Society in awarding him the 2002 Oersted Medal for “Reformulating the Mathematical Language of Physics” [9]. Yet even with this endorsement GA remains obscure, acceptance confoundingly slow.

As shown in **figures 1 and 2** and discussed elsewhere[28], IA and GA share the same Pauli FGOs. Six geometric objects, three magnetic and three electric, follow from the electron model. However, the model yields not one but two electric flux quanta[11, 29].

The first is associated with the magnetic flux quantum (a fundamental constant) and quantization of magnetic flux in the photon, which by Maxwell’s equations requires quantization of electric flux as well. The second follows from applying Gauss’s law to the electron charge, and is a factor of 2α smaller, where α is the electromagnetic fine structure constant. Similarly, there are not one but two electric dipole moments in the model.

Like the wave function, whose ‘reality’ is of interest in quantum interpretations [30], FGOs of the 3D Pauli algebra are not observable. Of interest here are impedances of observables, taken to be impedances of *interactions* between Pauli FGOs - the mode impedances of the 4D Dirac algebra. Or if you will, the S-matrix elements de-

rived from the impedance representation.

The matrix elements of **figure 2**, grouped by geometric grade, comprise a 4D Dirac algebra of flat Minkowski spacetime, generated by taking geometric products of the Pauli FGOs. From these interactions time (relative phase) emerges, and topological symmetry is broken.

Topological Symmetry Breaking in GA

Given two vectors a and b , the geometric product ab mixes products of different dimension, or *grade* (**figure 3**). In the product $ab = a \cdot b + a \wedge b$, two 1D vectors have been transformed into a point scalar and a 2D bivector.

“The problem is that even though we can transform the line continuously into a point, we cannot undo this transformation and have a function from the point back onto the line...” [31]. This breaks both topological and time symmetry, and is presumably true for all grade/dimension increasing operations. The presence of the singularity is implicit, becomes explicit when we introduce the singularities of the impedance model.

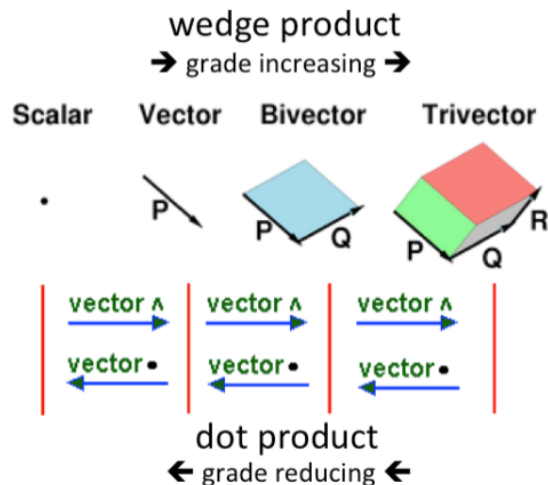


FIG. 3. Geometric algebra components in the 3D Pauli algebra of flat space. In GA the term grade is preferred to dimension, whose meaning in physics is sometimes ambiguous and confused with degrees of freedom. The two products (dot and wedge or inner and outer) that comprise the geometric product lower and raise the grade [32]

In the above example of the geometric product of two vectors, the number of singularities is not conserved. In the impedance model (**figure 1**) each vector is comprised of two singularities (those of the magnetic flux quantum of **figure 2** are at opposite infinities), for a total of four singularities entering the geometric product. Emerging from the product is a scalar electric charge (one singularity) and a pseudovector (none). In the process three singularities disappear.

In the impedance model scalars and vectors contain singularities, and their dual pseudovectors and pseudoscalars do not, a topological distinction between particle and pseudoparticle. It would seem that there are two types of topological symmetry breaking in this ex-

ample. One follows directly from dimensional transformations of the geometric product and the other from appearance and disappearance of singularities introduced by the impedance model. They are distinguished by the presence of an event horizon in the physical model.

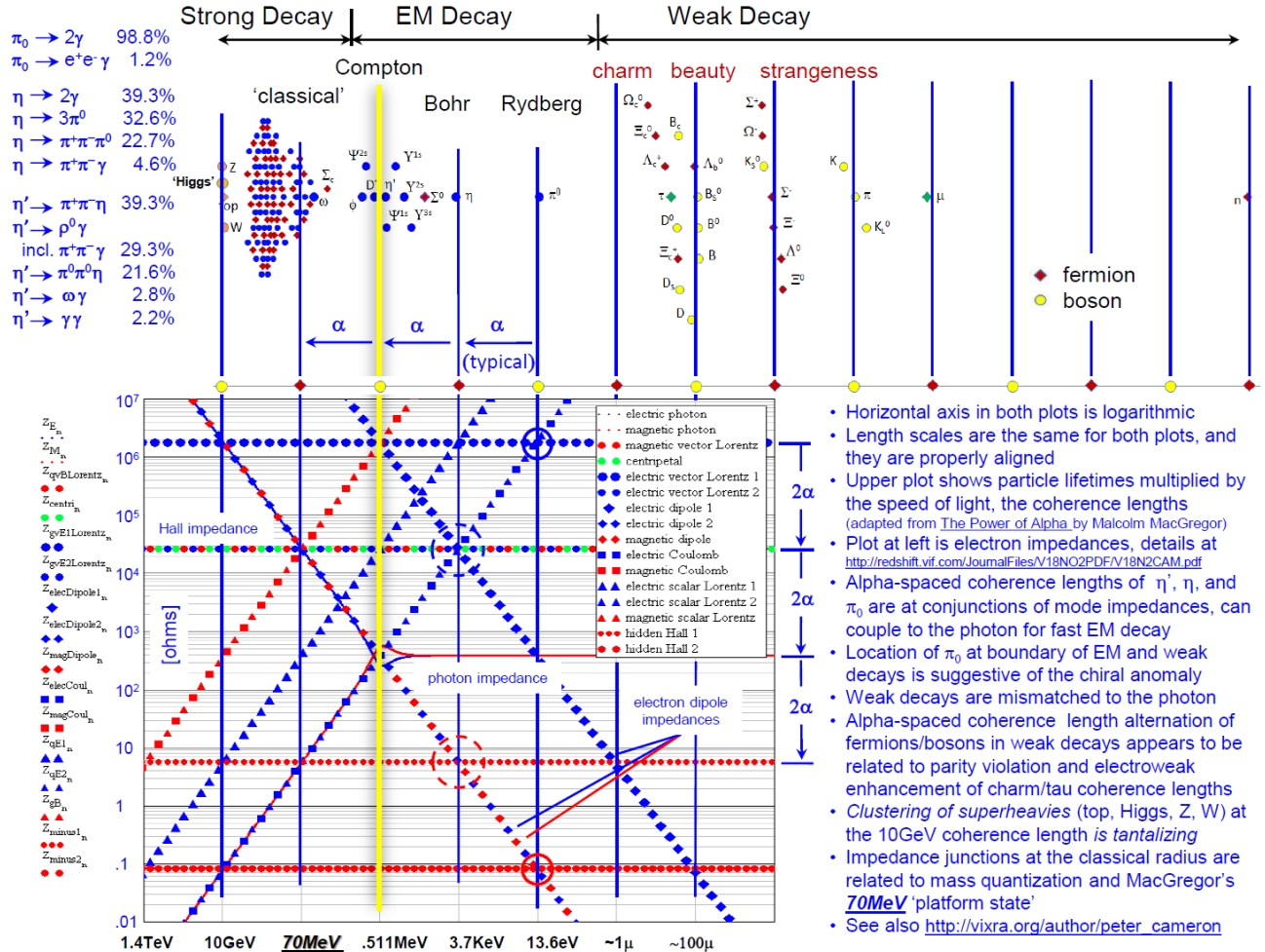


FIG. 4. In QFT one is permitted to define but one fundamental length (customarily taken to be the short wavelength cutoff). The impedance approach is finite, divergences being cut off by impedance mismatches as one moves away from the fundamental length of the model, the electron Compton wavelength. With FGOs of the model confined to that scale by the mismatches, interaction impedances can be calculated as a function of their separation, the ‘impact parameter’. Strong correlation of the resulting network nodes with unstable particle coherence lengths[33–37] follows from the requirement that impedances be **matched** for energy flow between modes as required by the decay process, permitting for instance precise calculation of π_0 , η , and η' branching ratios and resolution of the chiral anomaly[23].

S-MATRIX AND THE IMPEDANCE REPRESENTATION

Chapter 11 of Hatfield’s textbook [20] on the quantum field theory of point particles and strings opens with this statement of S-matrix universality:

“One of our goals in solving interacting quantum field theories is to calculate cross sections for scattering processes that can be compared with experiment. To compute a cross section, we need to know the S-matrix el-

ement corresponding to the scattering process. So, no matter which representation of field theory we work with, in the end we want to know the S-matrix elements. How the S-matrix is calculated will vary from representation to representation.”

Barut, in opening his comprehensive introduction[19], asks “What is the meaning of the S-matrix elements?” and answers “It is the *transition probability amplitude* from the initial state i to the final state f . It is in the use of probability amplitudes rather than probabilities that the quantum principle enters into the theory.”

In the process of decohering/collapsing the wave function, the amplitude is extracted and the phase is lost [38]. The use of *complex* transition probability amplitudes permits taking the product of the wave function with its conjugate, canceling the phase - the mathematical equivalent of decohering the physical wave function. Normalized this delivers the probability. In GA the Dirac algebra is a real algebra, and phase information is contained in the pseudoscalar \mathbf{I} .

Impedance may be defined as the amplitude and phase of opposition to the flow of energy. Whereas the S-matrix is comprised of complex probability amplitudes and phases, the impedance matrix is comprised of that which governs those amplitudes and phase shifts. The essential point, missing from QFT and crucially relevant in models and theories of quantum interactions, is this: **Impedances are quantized**. Yet how, if impedance quantization is both fact of nature and powerful theoretical tool, is it not already present in the Standard Model?

This absence is most remarkable. Impedance is a fundamental concept, universally valid. Impedance matching governs the flow of energy. The oversight can be attributed primarily to three causes. The first is historical [24], the second follows from the penchant of particle physicists to set fundamental constants to dimensionless unity, and the third from topological and electromagnetic paradoxes in our systems of units [11, 29, 39].

The **first** is a simple historical accident, a consequence of the order in which experimentalists revealed relevant phenomena. The scaffolding of QFT was erected on experimental discoveries of the first half of the twentieth century, on the foundation of QED, which was set long before the Nobel prize discovery of the scale invariant quantum Hall impedance in 1980 [40]. Prior to that impedance quantization was more implied than explicit in the literature [41–47]. The concept of *exact* impedance quantization did not exist.

A more prosaic **second cause** is the habit of particle physicists to set fundamental constants to dimensionless unity. Setting free space impedance to dimensionless unity made impedance quantization just a little too easy to overlook. And to no useful purpose. What matters are not absolute values of impedances, but rather their relative values, whether they are **matched**.

The **third confusion** is seen in an approach [43] summarized [44] as “...an analogy between Feynman diagrams and electrical circuits, with Feynman parameters playing the role of resistance, external momenta as current sources, and coordinate differences as voltage drops. Some of that found its way into section 18.4 of...” the canonical text [45]. As presented there, the units of the Feynman parameter are [sec/kg], the units not of resistance, but rather mechanical *conductance* [48].

It is not difficult to understand what led us astray [13, 43, 49–51]. The units of mechanical impedance are [kg/sec]. One would think that more [kg/sec] would mean

more mass flow. However, the physical reality is more [kg/sec] means more impedance and *less* mass flow. This is one of many interwoven mechanical, electromagnetic, and topological paradoxes [39] to be found in the SI system of units, which ironically were developed with the intent that they “...would facilitate relating the standard units of mechanics to electromagnetism.” [52].

With the confusion that resulted from misinterpreting conductance as resistance and lacking the concept of quantized impedance, the anticipated intuitive advantage [45] of the circuit analogy was lost. The possibility of the jump from a well-considered analogy to a photon-electron impedance model was not realized at that time.

Had impedance quantization been discovered in 1950 rather than 1980, one wonders whether it might have found its way into the foundation of QED at that time, before it was set in the bedrock. As it now stands the inevitable reconciliation of practical and theoretical, the incorporation of impedances into the foundations of quantum theory, opens new and exciting possibilities.

Transformation between impedance and scattering matrices is standard fare in electrical engineering[21, 53, 54]. There is nothing particularly difficult or mysterious about this. As we endeavor to make clear in this paper, when seeking to understand details of the elementary particle spectrum significant advantages accrue for the physicist working in the impedance representation.

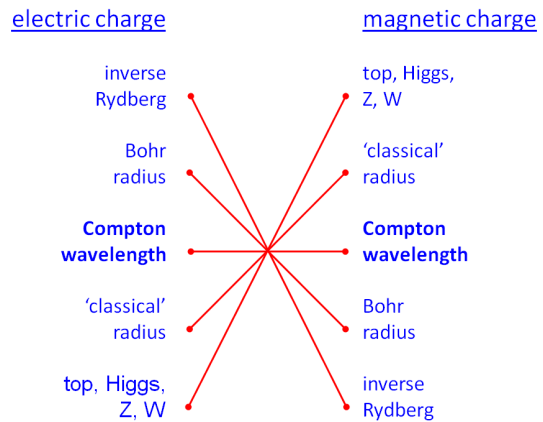


FIG. 5. Inversion of the fundamental lengths of **figure 4** by magnetic charge [55], with the magnetic singularity removed to infinity by the Dirac string [25].

DARK MODES AND SYMMETRY BREAKING

Much of the structure we observe in the physical world is organized around four fundamental interaction scales, ordered in powers of α - inverse Rydberg, Bohr radius, Compton wavelength, and classical electron radius (**figure 4**). The Compton wavelength $\lambda_e = h/m_e c$ contains no charge, is the same for both magnetic and electric charge (**figure 5**). However, substituting magnetic

charge for electric via the Dirac relation $2eg = h$ inverts the scaling of the remaining fundamental lengths [55].

With electric charge the lengths correspond to specific physical mechanisms of photon emission or absorption, matched in quantized impedance and energy. Inversion results in mismatches in both energy and impedance. Magnetic charge cannot couple directly to the photon

- not *despite* its great strength, but rather *because* of it.

Consequently the Dirac monopole is dark, cannot couple to the photon. The Bohr radius cannot be inside the Compton wavelength, Rydberg inside Bohr,... Specific physical mechanisms of photon emission and absorption no longer work. Related arguments can be advanced for the electric flux quantum and moment of **figure 1**.

	electric charge e scalar	electric moment 1 d_{E1} vector	electric moment 2 d_{E2} vector	mag flux quantum ϕ_B vector	elec flux quantum 1 ϕ_{E1} pseudovector	elec flux quantum 2 ϕ_{E2} pseudovector	magnetic moment μ_{Bohr} pseudovector	magnetic charge g pseudoscalar
e	ee scalar	ed_{E1}	ed_{E2} vector	$e\phi_B$	$e\phi_{E1}$	$e\phi_{E2}$ bivector	$e\mu_B$	eg pseudovector
d_{E1}	$d_{E1}e$	$d_{E1}d_{E1}$	$d_{E1}d_{E2}$	$d_{E1}\phi_B$	$d_{E1}\phi_{E1}$	$d_{E1}\phi_{E2}$	$d_{E1}\mu_B$	$d_{E1}g$
d_{E2}	$d_{E2}e$	$d_{E2}d_{E1}$	$d_{E2}d_{E2}$	$d_{E2}\phi_B$	$d_{E2}\phi_{E1}$	$d_{E2}\phi_{E2}$	$d_{E2}\mu_B$	$d_{E2}g$
ϕ_B	$\phi_B e$ vector	$\phi_B d_{E1}$	$\phi_B d_{E2}$ scalar + bivector	$\phi_B \phi_B$	$\phi_B \phi_{E1}$	$\phi_B \phi_{E2}$ vector + pseudovector	$\phi_B \mu_B$	$\phi_B g$ bivector
ϕ_{E1}	$\phi_{E1} e$	$\phi_{E1} d_{E1}$	$\phi_{E1} d_{E2}$	$\phi_{E1} \phi_B$	$\phi_{E1} \phi_{E1}$	$\phi_{E1} \phi_{E2}$	$\phi_{E1} \mu_B$	$\phi_{E1} g$
ϕ_{E2}	$\phi_{E2} e$	$\phi_{E2} d_{E1}$	$\phi_{E2} d_{E2}$	$\phi_{E2} \phi_B$	$\phi_{E2} \phi_{E1}$	$\phi_{E2} \phi_{E2}$	$\phi_{E2} \mu_B$	$\phi_{E2} g$
μ_B	$\mu_B e$ bivector	$\mu_B d_{E1}$	$\mu_B d_{E2}$ vector + pseudovector	$\mu_B \phi_B$	$\mu_B \phi_{E1}$	$\mu_B \phi_{E2}$ scalar + pseudoscalar	$\mu_B \mu_B$	$\mu_B g$ vector
g	ge pseudovector	gd_{E1}	gd_{E2} bivector	$g\phi_B$	$g\phi_{E1}$	$g\phi_{E2}$ vector	$g\mu_B$	gg scalar

FIG. 6. Modes lacking dark Pauli FGOs are highlighted, correspond to the transition (yellow) and eigenmodes (blue) of the stable proton. Unstable particles contain at least one dark FGO, the proton none. The differing interaction of dark and visible FGOs with the vacuum (essentially the virtual electron impedance network) determines the differing impedances they see [27]. This generates differential phase shifts, resulting in decoherence of unstable particles at impedance nodes (**figure 4**). The matrix is arranged in even (blue) and odd (yellow) by geometric grade of the emerging Dirac FGOs (the observables).

The electron model presented here starts with maximal electric-magnetic symmetry[12] in the 3D Pauli algebra of physical space. Electric and magnetic FGOs are taken to be duals. Scalar and pseudoscalar are duals, as are vector and pseudovector. The inversion of fundamental interaction scales of **figures 4 and 5** suggests that the duality is both electromagnetic and topological. Given that we define magnetic charge via the Dirac relation, which it-

self breaks topological symmetry, it is not surprising to find other manifestations of this symmetry breaking.

For example, the magnetic flux quantum $\phi = \frac{h}{2e}$ and magnetic charge as defined by the Dirac relation $g = \frac{h}{2e}$ are numerically equal, but topologically distinct [29].

Topological character is also suggested by the inversion of units of mechanical impedance - more [kg/sec] means more impedance and *less* mass flow.

As mentioned earlier, there are additional electromagnetic symmetry breakings. There is only one magnetic flux quantum, but two electric flux quanta. One magnetic moment, but two electric moments. How these might be related to topology is not yet clear.

In what follows the distinction between dark modes (whose presence dominates the impedance matrix of **figure 6**) and visible modes is utilized to identify the mode structure of the proton. With that and the symmetry breakings in hand, we seek to provide mechanisms for topological mass generation and possibilities for investigating proton structure and spin [1],...

PROTON MODE STRUCTURE

The electron is not a point particle. It gives that appearance if one doesn't appreciate the possibility that electron geometric structure, when endowed with electric and magnetic fields and excited by the photon, might generate the remainder of the massive particle spectrum. By far the lightest of all charged elementary particles, the electron impedance network is the natural candidate for this role [56], in some sense might be considered the structure of the vacuum [27]. We seek to understand details of how the stable proton emerges from excitation of that network (elsewhere we explore how a related approach sheds light upon the early Big Bang [57]).

To sort out the dynamics of the full impedance/S-matrix is a formidable computational task. The impedance network of **figure 4** is non-linear (plot is log-log) and presents only a small subset of the modes of **figure 6**. Scale-dependent impedances open the possibility of noiseless parametric mixing and amplification (whose connection to topological mass generation remains to be explored) [58, 59]. Topological effects in general are not clearly understood. Within these complexities one must iterate mode compositions, orientations, couplings and phases. The problem is far beyond resources available (particularly to independent researchers) for the present purpose.

However, restricting attention to modes containing only the 'visible' FGOs of **figure 1** gives us both transition modes and eigenmodes of the proton (the only known particle absent from **figure 4** - more on neutrinos later), resulting in tremendous simplification. Modes containing visible FGOs only are highlighted in green in **figure 6**.

The FGOs entering the geometric products to generate the transition modes are shown in **figure 7**, as well as grades of the FGOs emerging from the products and their corresponding identities in the impedance representation.

Transition Modes and Topological Mass

In the impedance approach there are two ways to calculate electron mass - from electromagnetic field energy of modes of the electron model [29], and from the impedance mismatch to the event horizon at the Planck length [60, 61]. Both methods are correct at the part-per-billion limit of experimental accuracy. Both require prior knowledge of the electron Compton wavelength, the input-by-hand fundamental length of the model.

Similarly, one can use either or both methods to calculate proton mass. And both require knowledge of the proton Compton wavelength, not a given in the model. The problem is how one makes the jump from electron Compton wavelength to that of the proton. This is where topological mass generation enters.

The muon mass calculation of the impedance approach agrees with experiment at one part per thousand, the pion at two parts per ten thousand, and the nucleon at seven parts per hundred thousand [29]. The muon and pion masses are calculated from field energies of flux quanta confined to the electron Compton wavelength. The nucleon calculation exploits the topological difference between Bohr magneton and flux quantum.

"It has been suggested that the origin of mass is somehow related to spin [13]. After the neutron, the next most stable particle is the muon. If we take the muon as a platform state [35] for the nucleon, in terms of spin-related phenomena we return here to the notion that the flux quantum is similar to a magnetic moment with no return flux, and consider the ratio of the magnetic flux quantum to the muon Bohr magneton

$$ratio_{\mu} = \frac{\phi_B}{\mu_{\mu Bohr}}$$

The nucleon mass can then be calculated as

$$m_{nucleonCalc} = \frac{\sqrt{2}}{2} \cdot e^2 \cdot ratio_{\mu}$$

where the $\frac{\sqrt{2}}{2}$ term might be regarded as a projection operator. Taking the measured nucleon mass to be the average of the proton and the neutron, we then have the calculated nucleon mass accurate to seven parts in one hundred thousand."[29]

Topological mass generation is a phenomenon in 2+1 dimensions in which Yang-Mills fields acquire mass upon the inclusion of a Chern-Simons term in the action [62], the essential point being that this happens without breaking gauge invariance, without losing quantum phase coherence. The phase shift of the added mass is compensated by that of the Chern-Simons term (whose mode impedance is scale invariant, and therefore shifts phase without emitting or absorbing energy).

In **figure 7** the Chern-Simons term $\phi_B e$ is the quantum Hall impedance of the charge ‘orbiting’ in the field of the flux quantum, the charge being driven by the electromagnetic fields of the impinging photon. The two spin zero (vectors have no spin) flux quanta ϕ_B are indistinguishable bosons, can be taken to couple the bivector (GA equivalent of a Yang-Mills axial vector) Bohr magneton μ_B to the charge scalar e .

transition mode FGOs			
mode	entering FGOs	emerging FGOs	E&M FGOs
$\phi_B e$	vector + scalar	vector	ϕ_B
$\phi_B \mu_B$	vector + pvector	vector + pscalar	$\phi_B + g$

FIG. 7. Transition modes of **figure 6** having only ‘visible’ FGOs entering the geometric products, and showing grades of emerging FGOs and the corresponding electromagnetic FGOs of the impedance model.

FGOs entering geometric products of the transition modes (left column of **figure 7**) number one scalar, two vectors, and one bivector. These comprise a minimally

complete geometric algebra in two spatial dimensions. Their geometric products yield two vector flux quanta ϕ_B and the pseudoscalar magnetic charge g . With the pseudoscalar we’ve gained a dimension. Via the interactions we have the 2+1 dimensions of topological mass generation [62]. This suggests the pseudoscalar can be identified with time, perhaps defines relative phases.

At the scale of the .511 MeV electron Compton wavelength there exist modes of the electron impedance model that are shifted in energy by powers of α , a consequence of nodes of the impedance network being arranged in such powers. Scalar Lorentz coupling of emergent magnetic charge g to flux quantum ϕ_B (rightmost column of **figure 7**) yields a route to the 70 MeV mass quantum, and a few pages later the muon mass [29].

In accord with that calculation, if one takes μ_B entering the interaction (leftmost column of **figure 7**) to be not the electron Bohr magneton but rather that of the muon and ϕ_B to be similarly confined to the muon Compton wavelength, then the energy of the bivector magneton in the field of the vector flux quantum, the energy of the $\phi_B \mu_B$ transition mode, is the muon mass.

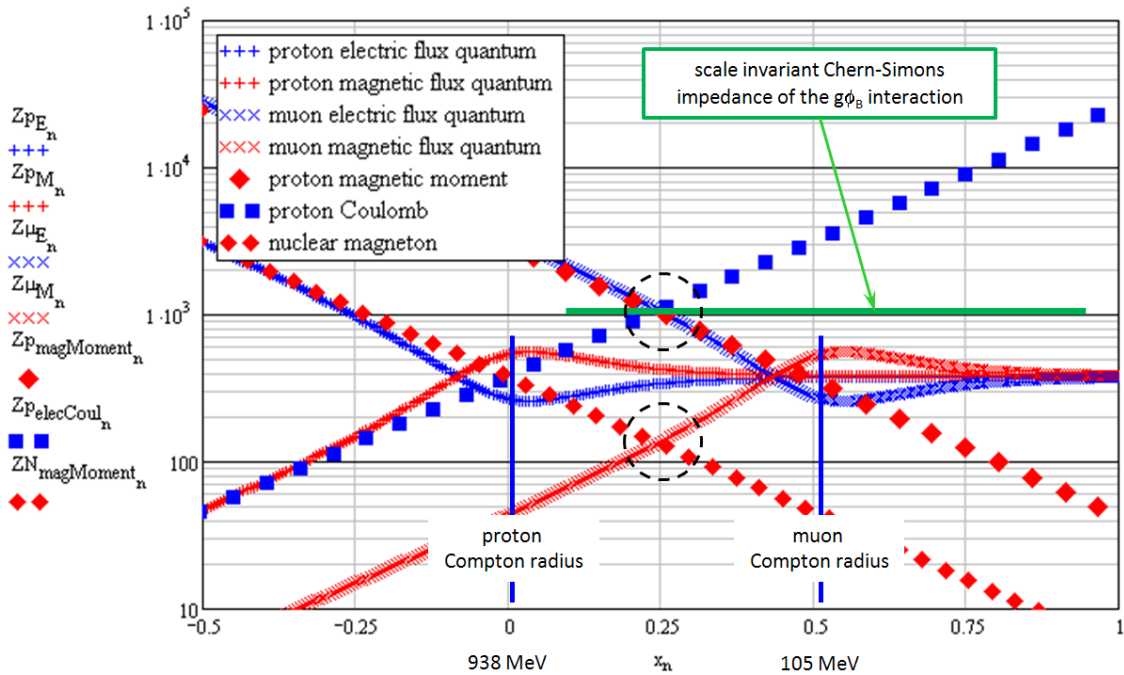


FIG. 8. Impedance network of muon-proton topological mass generation. Horizontal scale is photon wavelength/energy, logarithmic in powers of the fine structure constant α . Energy step from muon to proton is $\sim \sqrt{2}\alpha$.

One might suppose this a recipe for muon making. Muon lifetime/decoherence then derives from the differing impedances/phase shifts seen by the numerically equal but topologically distinct pseudoscalar charge g and vector flux quanta ϕ_B , the subtle topological distinction perhaps accounting for the exceptionally long muon lifetime.

According to this recipe, if one turns up the flame and continues cooking, given sufficient heat the proton emerges. How energy is transferred is shown in **figure 8**. The numerical identity between topologically distinct flux quantum ϕ_B and charge g is pivotal here. The 1027 ohm green line corresponds to the scale invariant Chern-Simons impedance of the three-body $\phi_B g \phi_B$

mode. It intersects the impedance node at the (logarithmic) midpoint between muon and proton. Also impedance matched at the node are the near field 105 MeV muon electric flux quantum, and the Coulomb and magnetic moment impedances of the proton. Coupling of energy from muon to proton is via the impedance match between the near field impedances of the muon electric flux quantum and proton magnetic moment bivectors and Coulomb scalars.

The point here is that the proton magnetic moment impedance plotted in the figure corresponds to the experimentally measured proton gyromagnetic ratio. Without the anomalous portion of the proton magnetic moment, topological mass generation doesn't work. As shown in the figure, the impedance corresponding to the anomaly-free nuclear Bohr magneton is that which matches the near field electrical impedance of the 938 MeV proton electric flux quantum (which is yet a few zeptoseconds in the future of topological mass generation), not that of the muon. The anomaly is essential.

However, the 938 MeV proton-mass $\mu_B\mu_B$ mode (figure 9) is not that of the measured moment, but rather the anomaly-free theoretical nuclear magneton! This suggests that the anomaly originates not in the proton, but rather in the transition excitation/measurement.

Proton Eigenmodes

The eigenmode Dirac FGOs emerging from the geometric products (figure 9) number three scalars, two bivectors, and one pseudoscalar - an even subalgebra of the Dirac algebra, itself again a Pauli algebra.

eigenmode FGOs			
mode	entering FGOs	emerging FGOs	E&M FGOs
ee	two scalars	scalar	e
$\phi_B\phi_B$	two vectors	scalar + pvector	$e + \mu_B$
$\mu_B e$	pvector + scalar	pvector	μ_B
$\mu_B\mu_B$	two pvectors	scalar + pscalar	$e + I$

FIG. 9. Eigenmodes of figure 6 having only visible Pauli FGOs entering the geometric products, and showing grades of emerging Dirac FGOs and the corresponding electromagnetic FGOs of the impedance model.

The connection of the emergent **three scalars** with quarks seems obvious. The only scalar in our model is electric charge. Given that the top and left Pauli algebras of figure 6 correspond to electron and positron 'wave functions', then all three scalars follow from three particle-antiparticle geometric products ($e\bar{e}$, $\phi_B\bar{\phi}_B$, and $\mu_B\bar{\mu}_B$), one for each of the three grades entering the products. All are found on the diagonal of the matrix of figure 6.

Also prominent on both the diagonal and the impedance network of figure 4 is the Coulomb mode $g\bar{g}$ of magnetic charge, part of the mode structure of the superheavies (top, Higgs, Z, W,...).

The first 'quark', the scalar e emerging from the charge pair $e\bar{e}$, is unaccompanied. One wonders if it is in any observable way different from the second, emerging from the $\phi_B\bar{\phi}_B$ interaction in the company of the pseudovector μ_B , or whether they are distinguishable from the third, emerging from $\mu_B\bar{\mu}_B$ along with pseudoscalar I .

The two bivector pseudovectors μ_B emerging from the geometric products $\phi_B\bar{\phi}_B$ and $\mu_B e$ might be identified with axial vectors of Yang-Mills theory. As mentioned in the previous sub-section, the 938 MeV proton rest mass of the emergent coupled $\mu_B\bar{\mu}_B$ mode corresponds to the interaction energy **not** of the measured magnetic moment, but rather the $g=2$ gyromagnetic ratio of the nuclear magneton.

The grade-4 **pseudoscalar** $I = \gamma_0\gamma_1\gamma_2\gamma_3$ defines spacetime orientation as manifested in the phases, with γ_0 the sign of time orientation. The γ_μ are orthogonal basis vectors in the Dirac algebra of flat 4D Minkowski spacetime, not matrices in 'isospace'. [10]

There are no gluons or weak vector bosons to bind the constituents. The modes are confined by the impedance mismatches, by reflections as one moves away from the quantization scales as defined by the impedance nodes. Mismatches also remove infinities associated with singularities. The impedance approach is finite and confined.

Proton Spin

Neither scalar (one singularity) nor vector (two) has intrinsic spin, but rather only the bivector (and possibly higher grade geometric objects), taken in the literature to be a magnetic flux quantum and given the attribute of a spin 1/2 fermion [63]. However magnetic geometric grades are inverted relative to electric by the topological duality. It is not magnetic flux quantum, but rather magnetic moment, that is to be identified with the bivector spin 1/2 fermion, an assignment in agreement with Jackson as well [64] (who persisted in calling it a dipole despite the absence of poles/singularities).

If one takes that moment to be in some sense not a vector dipole but rather a pseudovector dipole comprised of two pseudoscalar magnetic charge volume elements, then the proton angular momentum controversy arising from trying to 'locate' the intrinsic *exact* half-integer spin [4] need no longer be portioned out to various inexact origins, but rather might find resolution in the diffuse singularity-free character of such a magnetic moment.

To understand dynamics of proton spin more deeply will likely require further application of GA, and particularly the rotor, to the impedance model.

SUMMARY AND CONCLUSION

The serendipitous commonality of fundamental geometric objects between the impedance model and geometric Clifford algebra lends a formal structure to the impedance approach that maximizes the utility of both, providing simple yet powerful mathematical tools to the physicist and physical intuition to the mathematician.

Thus far applications of generalized quantum impedances have been primarily conceptual, limited to theoretical particle physics, quantum gravity, and quantum information theory. Sage advice [65] suggests that the most fertile field for impedances will be in condensed matter - in atomic, molecular, and optical physics, and particularly in superconductivity. If there is practical value in this, AMO is the place where it will be found. Though harking back to Wheeler [14], impedance matching might prove equally useful in understanding both fission and fusion.

ACKNOWLEDGEMENTS

The author thanks

- Michaele Suisse for many helpful discussions and literature searches/compilations/networking/...
- John Nees of the University of Michigan ultrafast high energy laser lab for helpful discussions and references,
- David Hestenes for the amazing gift of *geometric* Clifford algebra, and
- Yannis Semertzidis for ideas and encouragement during early phases of this work.

We are but protons, neutrons, and electrons. How this is possible will ever be the mystery of infinite gratitude.

* electronGaugeGroup@gmail.com

- [1] A.D. Krisch, "Collisions of Spinning Protons", *Sci. Am.* **257** 42 (1987)
- [2] S. Bass, "The Spin Structure of the Proton", *RMP* **77** 1257-1302 (2005)
<http://arxiv.org/abs/hep-ph/0411005>
- [3] C. Aidala et.al., "The Spin Structure of the Nucleon", *RMP* **85** 655-691 (2013)
<http://arxiv.org/abs/1209.2803>
- [4] E. Leader, "On the controversy concerning the definition of quark and gluon angular momentum", *Phys. Rev. D* **83** 096012 (2011)
- <http://arxiv.org/pdf/1101.5956v2.pdf>
- [5] H. Grassmann, *Lineale Ausdehnungslehre* (1844)
- [6] H. Grassmann, *Die Ausdehnungslehre*, Berlin (1862)
- [7] W. Clifford, "Applications of Grassmann's extensive algebra", *Am. J. Math* **1** 350 (1878)
- [8] D. Hestenes, *Space-Time Algebra*, Gordon and Breach, New York (1966)
- [9] D. Hestenes, "Oersted Medal Lecture 2002: Reforming the mathematical language of physics", *Am. J. Phys.* **71**, 104 (2003) <http://geocalc.clas.asu.edu/pdf/OerstedMedalLecture.pdf>
- [10] C. Doran and A. Lasenby, *Geometric Algebra for Physicists*, Cambridge University Press (2003)
- [11] P. Cameron, "Electron Impedances", *Apeiron* **18** 2 222-253 (2011) <http://redshift.vif.com/JournalFiles/V18N02PDF/V18N2CAM.pdf>
- [12] E. Witten, "Duality, Spacetime, and Quantum Mechanics", *Physics Today*, p.28-33 (May 1997)
- [13] P. Cameron "The Two Body Problem and Mach's Principle", submitted to *Am. J. Phys.* (1975), in revision. The original was published as an appendix to [11].
- [14] J. Wheeler, "On the Mathematical Description of Light Nuclei by the Method of Resonating Group Structure", *Phys. Rev.* **52** 1107-1122 (1937)
- [15] W. Heisenberg, "Die beobachtbaren Grossen in der Theorie der Elementarteilchen. I", *Z. Phys.* **120** (710): 513-538 (1943)
- [16] W. Heisenberg, "Die beobachtbaren Grossen in der Theorie der Elementarteilchen. II". *Z. Phys.* **120** (1112): 673-702 (1943)
- [17] W. Heisenberg, "Die beobachtbaren Grossen in der Theorie der Elementarteilchen. III". *Z. Phys.* **123** 93-112 (1944)
- [18] G. Chew, *S-matrix Theory of Strong Interactions*, (1961)
- [19] A.O. Barut, *The Theory of the Scattering Matrix for Interactions of Fundamental Particles*, McMillan (1967)
- [20] D. Hatfield, *Quantum Field Theory of Point Particles and Strings*, Addison-Wesley (1992)
- [21] for those unfamiliar with the scattering matrix, a simple introduction to a two port network showing both impedance and scattering representations is available http://www.antennamagus.com/database/utilities/tools_page.php?id=24&page=two-port-network-conversion-tool
- [22] P. Cameron, "Generalized Quantum Impedances: A Background Independent Model for the Unstable Parti-

- cles" (2012) <http://arxiv.org/abs/1108.3603>
- [23] P. Cameron, "An Impedance Approach to the Chiral Anomaly" (2014) <http://vixra.org/abs/1402.0064>
- [24] P. Cameron, "Historical Perspective on the Impedance Approach to Quantum Field Theory" (Aug 2014) <http://vixra.org/abs/1408.0109>
- [25] P. Dirac, "Quantized Singularities in the Electromagnetic Field", Proc. Roy. Soc. **A 133**, 60 (1931)
- [26] P. Dirac, "The Theory of Magnetic Poles", Phys. Rev. **74**, 817 (1948)
- [27] M. Urban et.al, "The quantum vacuum as the origin of the speed of light", Eur. Phys. J. D **67**:58 (2013)
- [28] P. Cameron, "E8: A Gauge Group for the Electron?" (Oct 2015) <http://vixra.org/abs/1510.0084>
- [29] P. Cameron, "Magnetic and Electric Flux Quanta: the Pion Mass", Apeiron **18** 1 p.29-42 (2011) <http://redshift.vif.com/JournalFiles/V18N01PDF/V18N1CAM.pdf>
- [30] M. Suisse and P. Cameron, "Quantum Interpretation of the Impedance Model", accepted for presentation at the 2014 Berlin Conf. on Quantum Information and Measurement. <http://vixra.org/abs/1311.0143>
- [31] R. Conover, A First Course in Topology: An Introduction to Mathematical Thinking, p.52, Dover (2014)
- [32] A useful visual introduction to geometric algebra can be found here <https://slehar.wordpress.com/2014/03/18/clifford-algebra-a-visual-introduction/>
- [33] M. H. MacGregor, "The Fine-Structure Constant as a Universal Scaling Factor", Lett. Nuovo Cimento **1**, 759-764 (1971)
- [34] M. H. MacGregor, "The Electromagnetic Scaling of Particle Lifetimes and Masses", Lett. Nuovo Cimento **31**, 341-346 (1981)
- [35] M. H. MacGregor, The Power of Alpha, World Scientific (2007) see also <http://137alpha.org/>
- [36] C. Capps, "Near Field or Far Field?", Electronic Design News, p.95 (16 Aug 2001) <http://edn.com/design/communications-networking/4340588/Near-field-or-far-field->
- [37] The mathcad file that generates the impedance plots is available from the author.
- [38] P. Cameron, "Quantum Impedances, Entanglement, and State Reduction" (2013) <http://vixra.org/abs/1303.0039>
- [39] P. Cameron, "The 'One Slide' Introduction to Generalized Quantum Impedances", p.42-43 <http://vixra.org/abs/1406.0146>
- [40] K. von Klitzing et.al, "New method for high-accuracy determination of the fine-structure constant based on quantized Hall resistance", PRL **45** 6 494-497 (1980)
- [41] J.L. Jackson and M. Yovits, "Properties of the Quantum Statistical Impedance", Phys. Rev. **96** 15 (1954) <http://www.deepdyve.com/lp/american-physical-society-aps/properties-of-the-quantum-statistical-impedance-8qnQk0mK33>
- [42] R. Landauer, "Spatial Variation of Currents and Fields Due to Localized Scatterers in Metallic Conduction", IBM J. Res. Dev. **1** 223 (1957) <http://citeseerx.ist.psu.edu/viewdoc/download?doi=10.1.1.91.9544&rep=rep1&type=pdf>
- [43] J. Bjorken, "Experimental tests of quantum electrodynamics and spectral representations of Green's functions in perturbation theory", Thesis, Dept. of Physics, Stanford University (1959) <http://searchworks.stanford.edu/view/2001021>
- [44] J. Bjorken, private communication (2014)
- [45] J. Bjorken, and S. Drell, Relativistic Quantum Fields, McGraw-Hill, section 18.4 (1965)
- [46] R. Feynman and F. Vernon, "The Theory of a General Quantum System Interacting with a Linear Dissipative System", Annals of Physics **24** 118-173 (1963) <http://isis.roma1.infn.it/~presilla/teaching/mqm/feynman.vernon.1963.pdf>
- [47] R. Landauer, "Electrical Resistance of Disordered One-dimensional Lattices", Philos. Mag. **21** 86 (1970)
- [48] N. Flertcher and T. Rossing, The Physics of Musical Instruments, 2nd ed., Springer (1998)
- [49] C. Lam, "Navigating around the algebraic jungle of QCD: efficient evaluation of loop helicity amplitudes", Nuc. Phys. B **397**, (12) 143172 (1993)
- [50] C. Bogner, "Mathematical aspects of Feynman Integrals", PhD thesis, Mainz (2009)
- [51] D. Huang, "Consistency and Advantage of Loop Regularization Method Merging with Bjorken-Drells Analogy Between Feynman Diagrams and Electrical Circuits", EJP C, (2012) <http://arxiv.org/abs/1108.3603>
- [52] M. Tobar, "Global Representation of the Fine Structure Constant and its Variation", Meteorologia **42** p.129-133 (2005)
- [53] https://en.wikipedia.org/wiki/Scattering_parameters
- [54] https://en.wikipedia.org/wiki/Impedance_parameters
- [55] T. Datta, "The Fine Structure Constant, Magnetic Monopoles, and the Dirac Quantization Condition", Lettere Al Nuovo Cimento **37** 2 p.51-54 (May 1983)

- [56] P. Cameron, “Quantizing Gauge Theory Gravity”, Barcelona conference on applications of geometric Clifford algebra (2015) <http://www-ma2.upc.edu/agacse2015/3641572286-EP/>
also available at <http://vixra.org/abs/1506.0215>
- [57] P. Cameron, “The First Zeptoseconds: An Impedance Template for the Big Bang (2015)
<http://vixra.org/abs/1501.0208>
- [58] W. Louisell, “Coupled Modes and Parametric Electronics”, Wiley (1960)
- [59] B. Zeldovich, “Impedance and parametric excitation of oscillators”, *Physics-Uspekhi* **51** (5) 465-484 (2008)
- [60] P. Cameron, “Background Independent Relations between Gravity and Electromagnetism”
<http://vixra.org/abs/1211.0052>
- [61] P. Cameron, “A Possible Resolution of the Black Hole Information Paradox”, Rochester Conference on Quantum Optics, Information, and Measurement (2013)
<http://www.opticsinfobase.org/abstract.cfm?URI=QIM-2013-W6.01>
also available at <http://vixra.org/abs/1304.0036>
- [62] S. Deser, R. Jackiw, and S. Templeton, “Three-Dimensional Massive Gauge Theories”, *PRL* **48** 975 (1982)
- [63] F. Wilczek, “Fractional Statistics and Anyon Superconductivity”, p.7 World Scientific (1990).
- [64] J.D. Jackson, “The Nature of Intrinsic Magnetic Dipole Moments”, CERN 77-17 (1977).
- [65] G. Kane, private communication (2014)